Soil Biology and Biochemistry 185 (2023) 109155

Contents lists available at ScienceDirect

Soil Biology and Biochemistry

journal homepage: www.elsevier.com/locate/soilbio

Revegetation promotes soil mineral-associated organic carbon sequestration and soil carbon stability in the Tengger Desert, northern China

Yunfei Li [a,b,1], Xue Zhang [a,1], Bingyao Wang [a], Xudong Wu [c], Zhanjun Wang [c], Lichao Liu [a,b], Haotian Yang [a,b,*]

[a] Shapotou Desert Research and Experiment Station, Northwest Institute of Eco-Environment and Resources, Chinese Academy of Sciences, Lanzhou, 730000, China
[b] University of Chinese Academy of Sciences, Beijing, 101408, China
[c] Institute of Forestry and Grassland Ecology, Ningxia Academy of Agricultural and Forestry Sciences, Yinchuan, 750002, China

A R T I C L E I N F O

Keywords:
Soil mineral-associated organic carbon
Particulate organic carbon
Soil carbon fraction
Revegetation
Microbial community

A B S T R A C T

Ecological restoration is considered an effective strategy for increasing soil carbon storage and mitigating climate change. However, the impact of revegetation in desert areas on the stability of soil organic carbon (SOC) is still unclear. We investigated the content and stability of SOC in restoration sites along a chronosequence in the Tengger Desert, focusing on the mineral-associated organic carbon (MAOC) and particulate organic carbon (POC) fractions. The content of SOC significantly increased with site age from 0.37 g kg^{-1} at year 0–5.32 g kg^{-1} at year 66. Revegetation significantly changed the SOC fraction and improved SOC stability as a factor of site age. In the 66-year-old site, the levels of MAOC and POC were increased by 255.67 and 9.24 times, respectively. The percentage of MAOC was increased from 1.50% to 28.92%, whereas that of POC was decreased from 98.50% to 71.08%. Based on our findings, the content and proportion of MAOC and POC are closely related to plant input, soil variables, and the soil microbial community. We estimate that the maximum content and proportion of MAOC are 2.65 g kg^{-1} and 36.71% with continuous succession, based on the soil clay and silt contents. Overall, revegetation improved the stability of SOC. Our study highlights the importance of the revegetation of temperate desert areas to further mitigate climate change.

1. Introduction

Drylands account for approximately 45% of the global terrestrial area (Schimel, 2010). The desertification, soil and vegetation degradation in arid areas caused by climate change and human factors have affected about 11.37 10^8 ha soil and 25.76 10^8 ha rangeland vegetation (Lal, 2001), seriously threatening ecological security and human survival. In this context, vegetation restoration is recognized as the most effective measure to control desertification and restore soil (Le Houérou, 2000; Li et al., 2022a, 2022b). It has been estimated that afforestation in suitable drylands (4.48 10^8 ha) could lead to a total of 32.3 Gt net cumulative carbon (C) sequestration for a period of 80 years (2020–2100) (Rohatyn et al., 2022). Since the 1950s, the impact of vegetation restoration on soil C pools has been attracting considerable attention (Lal, 2004; Nosetto et al., 2006; Cunningham et al., 2012; Zhang et al., 2021), and it has become a consensus that the amount of soil C increases substantially after revegetation (Nosetto et al., 2006; Cunningham et al., 2012; Yang et al., 2014; Li et al., 2020, 2022a, 2022b). However, the effects of vegetation restoration on soil C stability and the underlying mechanisms are still largely unclear, impeding accurate estimates of soil C storage and balance.

The stability of the soil organic carbon (SOC) pool is determined by the different C fractions, which have different protective mechanisms and turnover rates (Christensen, 1996; Smith et al., 2002; Yu et al., 2022). The physical separation of SOC into particulate organic C (POC) and mineral-associated organic C (MAOC) is a popular classical approach and the basis for understanding the responses of SOC formation and persistence to environmental changes (Cotrufo et al., 2019;

* Corresponding author. Shapotou Desert Research and Experiment Station, Northwest Institute of Eco-Environment and Resources, Chinese Academy of Sciences, Lanzhou, 730000, China.
E-mail address: yanghaotian6516@163.com (H. Yang).
[1] These authors contributed equally to this work.

https://doi.org/10.1016/j.soilbio.2023.109155
Received 27 December 2022; Received in revised form 15 August 2023; Accepted 17 August 2023
Available online 21 August 2023

Witzgall et al., 2021; Heckman et al., 2022). The POC is largely composed of structural polymeric compounds of partially decomposed plant residues (Baldock and Skjemstad, 2000; Haddix et al., 2020), and biochemical resistance and physical protection are the main factors determining POC persistence (Lavallee et al., 2020; Witzgall et al., 2021). However, microbial necromass and metabolites are the major C sources of MAOC (Cotrufo et al., 2013; Liang et al., 2017), and these low-molecular-weight organic compounds are generally thought to form MAOC via "direct sorption pathway" with mineral particles or via the "*in vivo* microbial turnover pathway" (Sokol et al., 2019). The POC and MAOC differ in their biogeochemical properties and turnover rates due to their different sources and mechanisms of physicochemical protection (Lavallee et al., 2020). The microbial efficiency-matrix stabilization (MEMS) hypothesis and a growing body of evidence suggest that microbial processing of high-quality substrates results in more MAOC than low-quality ones (Cotrufo et al., 2013; Cyle et al., 2016; Lavallee et al., 2018), and MAOC stores more microbial necromass than POC (Griepentrog et al., 2014; Angst et al., 2019). Consequently, the MAOC decomposition rate is lower than that for POC, and MAOC generally has a longer residence time (decades–centuries) than POC (years–decades) (Kleber et al., 2015). Because of this, MAOC can be used as an important functional pool for long-term SOC sequestration (Sokol and Bradford, 2019). Grasping the dynamics of the content and distribution of POC and MAOC, and their driving forces, is the key to understand the impacts of revegetation on soil C pool stability.

The formation and decomposition of SOC fractions are closely related to plant inputs, soil physicochemical properties, and soil microbial activities (Golchin et al., 1994; Kögel-Knabne et al., 2008; Kramer et al., 2012; Kalbitz and Kaiser, 2008; Cotrufo et al., 2019; Angst et al., 2021). Plant input and compounds with low N contents dominate POM (Golchin et al., 1994), whereas MAOC is largely composed of N-rich microbial products (Kögel-Knabner et al., 2008). Soil texture affects MOAC formation via controlling the amount of mineral surface area available for binding (Kögel-Knabner et al., 2008; Haddix et al., 2020). Cotrufo et al. (2019) found that the SOC fraction and SOC stock were significantly related to land cover type, soil properties, and net primary production. In the past decades, although many studies investigated the changes in soil C pools during vegetation restoration (Nosetto et al., 2006; Cunningham et al., 2012; Poeplau and Don, 2013; Yang et al., 2014; Yu et al., 2017; de Moraes Sá et al., 2018; Li et al., 2022a, 2022b), only few studies revealed the effects of vegetation restoration on soil C pools stability from the perspective of C fractions. The biological and environmental factors driving the changes in SOC fractions, and the underlying mechanisms, are still largely unclear. With extreme climate events caused by global climate change (Abiodun et al., 2017), vegetation type and dominant species may change, and soil C may be re-released into the atmosphere (Bachelet et al., 2001; Chaturvedi et al., 2011; Li et al., 2022a, 2022b). The magnitude of this potential is closely related to SOC stability and fractional characteristics. As POC dominates heterotrophic respiration (Elliott, 1986; Arevalo et al., 2012), it can predict short-term SOC decomposition (Alvarez and Alvarez, 2000). In cases where a large MAOC pool compensates for POC with a relatively low decomposition rate, MAOC can also largely contribute to SOC decomposition (Christensen, 1987). With vegetation succession, the dynamic changes in the relative contents of POC and MAOC alter the stability of SOC. Therefore, comprehending the responses of the different C fractions with different stability levels to revegetation can deepen our understanding of ecological restoration.

Hence, based on a chronosequence of revegetation sites on the southeastern edge of the Tengger Desert, China, our objectives were to (1) investigate the effects of revegetation on various SOC fractions and the C pool size and (2) evaluate how revegetation influences SOC composition, accumulation, and stabilization by integrating plant input, soil properties, and microbial communities. We hypothesized that (1) the higher litter mass input induced by revegetation increases microbial biomass and its contribution to SOC via reducing nutrient limitation, thereby facilitating microbial growth, and (2) revegetation will increase MAOC formation, thereby improving SOC stabilization and enhancing long-term C sequestration in soils due to increased clay and silt levels and a higher number of microorganisms. The results of this study can facilitate a deeper understanding of the effects of revegetation efforts on soil C cycling and accumulation and enable us to predict the effects of long-term ecological restoration on SOC pools stabilization and soil C sequestration potential.

2. Materials and methods

2.1. Site description

The study area was located in the Shapotou region on the southeastern edge of the Tengger Desert, China (37°32′ N, 105°02′ E, 1339 m a.s.l) (Fig. 1). Average annual temperature is 10 °C, with a minimum of −25.1 °C in January and a maximum of 38.1 °C in July. Average annual precipitation is 186.2 mm, with an annual potential evapotranspiration of approximately 3000 mm. The soil is classified as wind-borne sand (FAO-ISRIC-ISSS, 1998; Yang et al., 2020), which is loose, infertile, and prone to erosion. Natural vegetation covers less than 1% of the area, and rainfall is the only water resource for plant growth and development. The mobile sand dune vegetation is dominated by *Hedysarum scoparium* Fisch., *Agriophyllum squarrosum* Moq., and *Stilpnolepis centiflora* (Maxim.) Krasch.

A non-irrigated, artificial sand-binding vegetation protection system (ecological restoration area) began to be constructed in 1956 to protect the Lanzhou-Baotou railway from sand burial. At first, straw checkerboard sand barriers (measuring 1 × 1 m) were built on mobile sand dunes, and subsequently, native shrub seedlings were planted within the straw checkerboard at a density of 16 individuals per 100 m^2. To enable long-term in situ observation and research, the vegetated area was further expanded along a south-north direction through the same approach in 1964, 1973, 1987, 1999, and 2011. At present, an ecological recovery area (16 km long and 700 m wide) with a chronosequence is being formed (Li et al., 2007). After the establishment of the vegetation protection system, herbaceous plant species gradually colonized the area, and biological soil crusts (BSCs) started to develop (such as cyanobacteria-, algae-, lichen-, and moss-dominated crusts). At 66 years after the establishment of the protection system, more than 10 herb species occurred in this area, with a vegetation coverage of 50%. The vegetation pattern gradually transformed from single-shrub community to a complex community of shrubs and herbs (Li et al., 2016). The plant types include semi-shrubs, shrubs, forbs, and grasses, such as *Artemisia ordosica* Krasch, *Caragana korshinskii* Kom, *H. scoparium* Fisch., *Eragrostis minor* Host, *Setaria viridis* (L.) Beauv., *Chloris virgata* Sw., *Bassia dasyphylla* (Fisch. Et Mey.) O. Kuntze, and *A. capillaris* Thunb.

2.2. Site selection and soil sampling preparation

Five sites along the chronosequence were selected for this study in 2022, namely four revegetation sites established in 1956 (66 y, stand age hereinafter), 1973 (49 y), 1987 (35 y), and 2011 (11 y), along with a mobile sand dune as control site (0 y). In July 2022, three sampling plots (10 × 10 m) were established at each of the five sites, and three intact soil cores (5 cm in diameter and 0–10 cm in depth) were obtained randomly from each plot to estimate fine root biomass. Within each plot, three subplots (1 × 1 m) were selected randomly for litter mass investigation; briefly, the litter was collected from the soil surface and taken to the laboratory, where it was oven-dried at 65 °C for 48 h and subsequently weighted.

One composite soil sample (about 0.5 kg) was prepared from each plot by thoroughly mixing 10 topsoil samples (0–10 cm) which were collected with a soil auger (5 cm inner diameter) in a random S-shaped pattern across the sample area, and a total of 15 composite samples were obtained. Each composite sample was sieved through a 2-mm mesh to

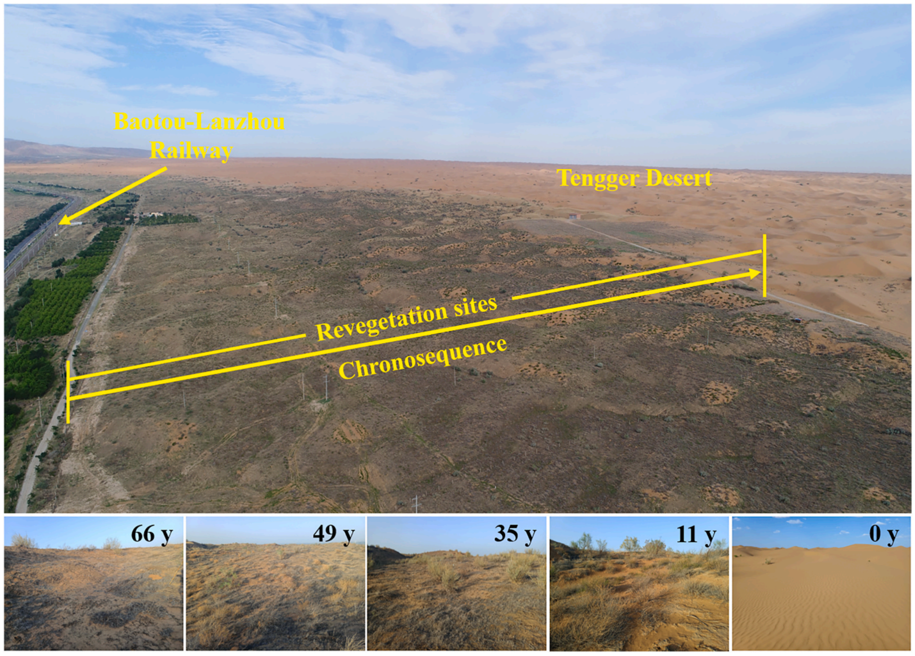

Fig. 1. General view of the research sites. The top panel shows the vegetation protection system of the Baotou-Lanzhou Railway, 0 y represents mobile sand dune site; 11 y, 35 y, 49 y and 66 y represent vegetation established in 2011, 1987, 1973 and 1956, respectively.

remove any recognizable plant material and then divided into two parts. The first part was stored at −20 °C for the analysis of the soil microbial community composition, and the other part was air-dried at room temperature for the analysis of SOC fractions and physicochemical properties. Additionally, bulk soil density (BD) was determined by collecting three replicate soil cores using steel cylinders (5.5 cm in diameter and 4.2 cm in height).

Fine root (<2 mm diameter) biomass was collected and estimated from nine soil cores per site by weighing all living roots. Root samples were picked from the soil, cleaned, and dried to constant weight at 65 °C. In addition, three square litter collectors with an area of 1 m^2 and a height of 0.2 m were randomly placed at each site to collect aboveground litterfall from mid-August 2021 to mid-August 2022. All litter samples were dried to constant weight at 65 °C.

2.3. SOC fraction and soil sample analyses

A classic method was used to determine POC and MAOC fractions, based on the size following chemical dispersion of aggregates (Cambardella and Elliott, 1992; Cotrufo et al., 2019). Briefly, 20 g of air-dried 2-mm-sieved soil was shaken in 100 mL sodium hexametaphosphate (0.5%) dispersing solution for 18 h. The dispersed soil samples were rinsed onto a 53-μm sieve, and the fraction remaining on the sieve (>53 μm) was defined as POC and that passing through it (<53 μm) was defined as MAOC. The fractions were oven-dried at 60 °C and pulverized, followed by analysis for C concentration in a total organic carbon analyzer (Vario TOC, Elementar, DE).

Soil particle-size distributions were determined by a laser diffraction analyzer (S3500, Microtrac Inc., Largo, FL, USA) after ultrasonic dispersal. The SOC content was determined by a total organic carbon analyzer (Vario TOC, Elementar, DE). The soil total nitrogen content (TN) was determined by a Kjeltec System (2300, Foss Inc., Hillerød, Denmark), and the total phosphorus content (TP) was measured colorimetrically after digestion with $HClO_4$–H_2SO_4.

Soil microbial community composition was characterized using phospholipid fatty acid (PLFA) analysis as described by Bossio and Scow (1998). In short, we used chloroform: methanol: citrate buffer (1:2:0.8, v: v: v) to extract lipids from 2 g of freeze-dried soil and subsequently separated the phospholipids from nonpolar lipids and converted them into fatty acid methyl esters (FAMEs). Each fatty acid was quantified by comparing the individual peak area with that of the internal standard (methyl nonadenoate; C19:0), and its quantity was expressed in nmol g^{-1} dry soil. The iso-, anteiso- (i13:0, i14:0, i15:0, a15:0, i16:0, i17:0 and a17:0), and 10Me- (10Me17:0 and 10Me18:0) branched PLFAs were used for Gram-positive bacteria (G+ bacteria) as representative markers of specific microbial groups; Gram-negative bacteria (G− bacteria) were investigated using monounsaturated and cyclopropyl PLFAs (17:1ω8c, 18:1ω5c, 18:1ω7c, cy17:0 and cy19:0) and fungi via 16:1ω5c, 18:1ω9c and 18:3ω6c PLFAs (Willers et al., 2015; Joergensen, 2021). The bacterial biomass was calculated as the sum of G+ and G-bacterial PLFAs; the sum of bacterial and fungal biomass was defined as the total microbial biomass.

2.4. Data analysis

Most statistical analyses were carried out using SPSS Statistics 21.0 for Windows (IBM Corp.). Statistically significant differences among sites were tested using one-way ANOVA followed by the least significant difference test at $p < 0.05$. Pearson's analysis was performed to examine the relationships among MAOC, POC, distribution of MAOC, plant input, soil variables, and soil microbial community. Based on the existing theory and the results of Pearson's correlation analysis, there is a fact that a robust maximum value of MAOC estimate can emerge as a function of only the content of clay and silt and the type of mineral (Haddix et al., 2020; Georgiou et al., 2022). Therefore, we first analyzed the relationship between stand age and content of clay and silt, and estimated the maximum content of clay and silt that continued to increase with stand age. Secondly, we quantitatively analyzed the relationship between the content and proportion of MAOC and clay and silt content, and then estimated the maximum content and proportion of MAOC according to the maximum content of clay and silt. As the content of MAOC and POC were altered by revegetation, plant input (litter mass and fine root biomass), soil variables (CS, BD, TN, TP, and C:N), and soil microbial (bacterial PLFAS and fungal PLFAs), the structural equation model (SEM) was fitted based on the known and potential relationships among different variables to investigate the direct and indirect effects of environmental factors on the responses of SOC fractions contents to restoration age, using the AMOS software (17.0). We chose the χ^2 test and the root mean square error (RMSE) of approximation to evaluate model fitness and sequentially optimized the SEMs until we attained the final model.

3. Results

3.1. Soil properties, litter mass, and fine root biomass

The levels of SOC, TN, TP, C: N ratio, clay and silt content, litter mass, and fine root biomass increased significantly along the chronosequence ($p < 0.05$), while those of BD and sand content decreased significantly ($p < 0.05$; Table 1, Fig. 2). The contents of SOC, TN, TP, C: N ratio, and clay and silt content increased by 13.38, 5.09,1.45,1.37, and 130.67 times, respectively, whereas those of BD and sand content had decreased by 8.44% and 15.70% after 66 years of revegetation (Table 1). In the sand dune, litter mass and fine root biomass were not investigated. After 66 years of revegetation, litter mass and fine root biomass were 10.11 and 2.69 g m^{-2}, respectively (Fig. 2).

3.2. Soil microbial community composition

Revegetation increased the amounts of total, bacterial, and fungal PLFAs as well as the fungal: bacterial PLFA ratio; the effects depended on the site age ($p < 0.05$; Fig. 3). In the sand dune, the levels of total, bacterial, and fungal PFLAs were 16.77, 5.76, and 1.43 nmol g^{-1}, respectively, and the fungal: bacterial PFLA ratio was 0.25. In the 66-year-old site, the levels of total, bacterial, and fungal PLFAs had increased by 54.85%, 70.53%, and 203.74% and the fungal: bacterial PFLA ratio by 78.29% (Fig. 3).

3.3. MAOC and POC

Revegetation increased the levels of MAOC and POC as well as the proportion of MAOC, but it decreased the proportion of POC ($p < 0.05$; Fig. 4). In the 0-year-old site (sand dune), the MAOC and POC levels were 0.006 and 0.369 g kg^{-1}, respectively. In the 66-year-old site, the levels of MAOC and POC had increased by 255.67 and 9.24 times, respectively (Fig. 4a). The proportions of MAOC and POC were 1.50% and 98.50% at 0 years and 28.92% and 71.08% at 66 years (Fig. 4b).

The rates of MAOC and POC sequestration were not significantly different across the sites; POC sequestration was generally more pronounced than MAOC sequestration. The MAOC and POC sequestration rates first increased and then decreased along the chronosequence. The levels were lowest in the 35-year-old site, namely 0.003 and 0.013 g kg^{-1} y^{-1}, respectively. The maximum levels were reached in the 49-year-old site with 0.043 and 0.117 g kg^{-1} y^{-1}, respectively (Fig. 4c).

Table 1
Soil properties of the research sites.

Properties	Stand age				
	0 y	11 y	35 y	49 y	66 y
SOC (g kg^{-1})	0.37 ± 0.01e	0.77 ± 0.04 d	3.01 ± 0.08c	4.42 ± 0.08 b	5.32 ± 0.04a
TN (g kg^{-1})	0.11 ± 0.01 d	0.16 ± 0.02 d	0.41 ± 0.02c	0.50 ± 0.04 b	0.67 ± 0.04a
TP (g kg^{-1})	0.11 ± 0.01e	0.14 ± 0.01 d	0.17 ± 0.01c	0.22 ± 0.00 b	0.27 ± 0.01a
BD (g cm^{-3})	1.54 ± 0.01a	1.52 ± 0.01a	1.48 ± 0.01 b	1.45 ± 0.01c	1.41 ± 0.01 d
C:N	3.35 ± 0.18 b	4.80 ± 0.40 b	7.41 ± 0.50a	8.95 ± 0.85a	7.94 ± 0.43a
Clay and silt content (%)	0.12 ± 0.03e	1.39 ± 0.45 d	8.49 ± 1.21c	11.97 ± 1.88 b	15.80 ± 1.77a
Sand content (%)	99.88 ± 0.03a	98.61 ± 0.45a	91.51 ± 1.21 b	88.03 ± 1.88c	84.20 ± 1.77 d

Note: values are mean ± SE. The different lowercase letters indicate significant differences at $p < 0.05$ level between the different stand age. SOC, soil organic carbon; TN, total nitrogen; TP, total phosphorus; BD, bulk density.

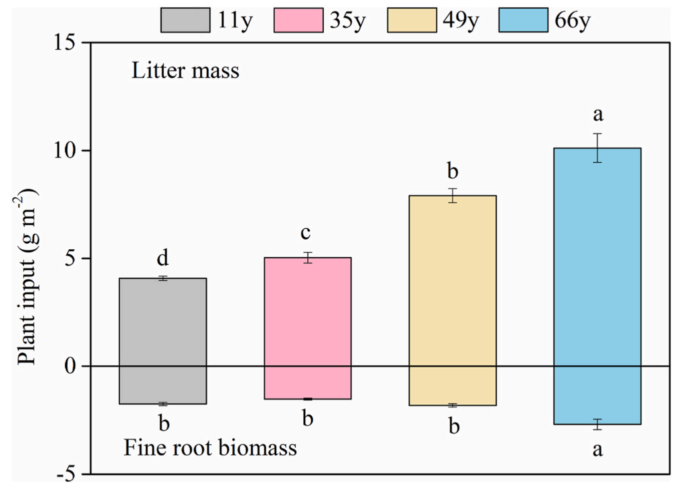

Fig. 2. Effect of revegetation on litter mass and fine root biomass. Error bars represent standard errors of the means (n = 3). Different letters indicate significant differences among stand age at $p < 0.05$.

3.4. Attribution analysis of MAOC and POC

The contents of MAOC and POC and the proportion of MAOC were positively correlated with litter mass, fine root biomass, clay and silt content, SOC, TN, TP, C: N ratio, total PLFAs, bacterial PLFAs, fungal PLFAs, and fungal: bacterial PLFA ratio and negatively with sand content and BD ($p < 0.01$; Table 2).

To identify and quantify the relationships between the contents of MAOC and POC and the environmental variables, we further performed SEM analysis. The SEM explained 96% and 98% of the variance in the content of MACO and POC, respectively (Fig. 5). Revegetation indirectly increased the content of MAOC by improving the soil quality and increasing the fungal PLFAs; the standardized total effects of soil and fungal PLFAs were 0.996 and 0.339. However, the fungal PLFAs and plant characteristics negatively affects the POC throughout the chronosequence with a standardized path coefficient of −0.58 and −0.20, respectively.

3.5. Maximum MAOC value

There was a non-linear relationship between clay and silt content with site age and between the proportion of MAOC with clay and silt content ($p < 0.001$; Fig. 6a and b). In contrast, MAOC was significantly linearly related to clay and silt content ($p < 0.001$; Fig. 6c). The maximum clay and silt content, the proportion of MAOC, and the MAOC were 27%, 36.71%, and 2.65 g kg^{-1} in the 0–10 cm soil with the extension of stand age, respectively.

4. Discussion

Revegetation in dryland is not only considered as an effective way to curb and reverse land desertification, but also an important way to mitigate global climate change because of its huge C sequestration potential (Bastin et al., 2019; Lewis et al., 2019; Rohatyn et al., 2022). Both the pros and cons of this approach have been widely reported. On the one hand, a large body of scientific research supports revegetation as an effective way to mitigating global warming. Firstly, revegetation is known to cool the local climate by increasing evaporation and inducing increased cloud formation and precipitation (Yosef et al., 2018; Rohatyn et al., 2022). Furthermore, Griscom et al. (2017) and Bastin et al. (2019)

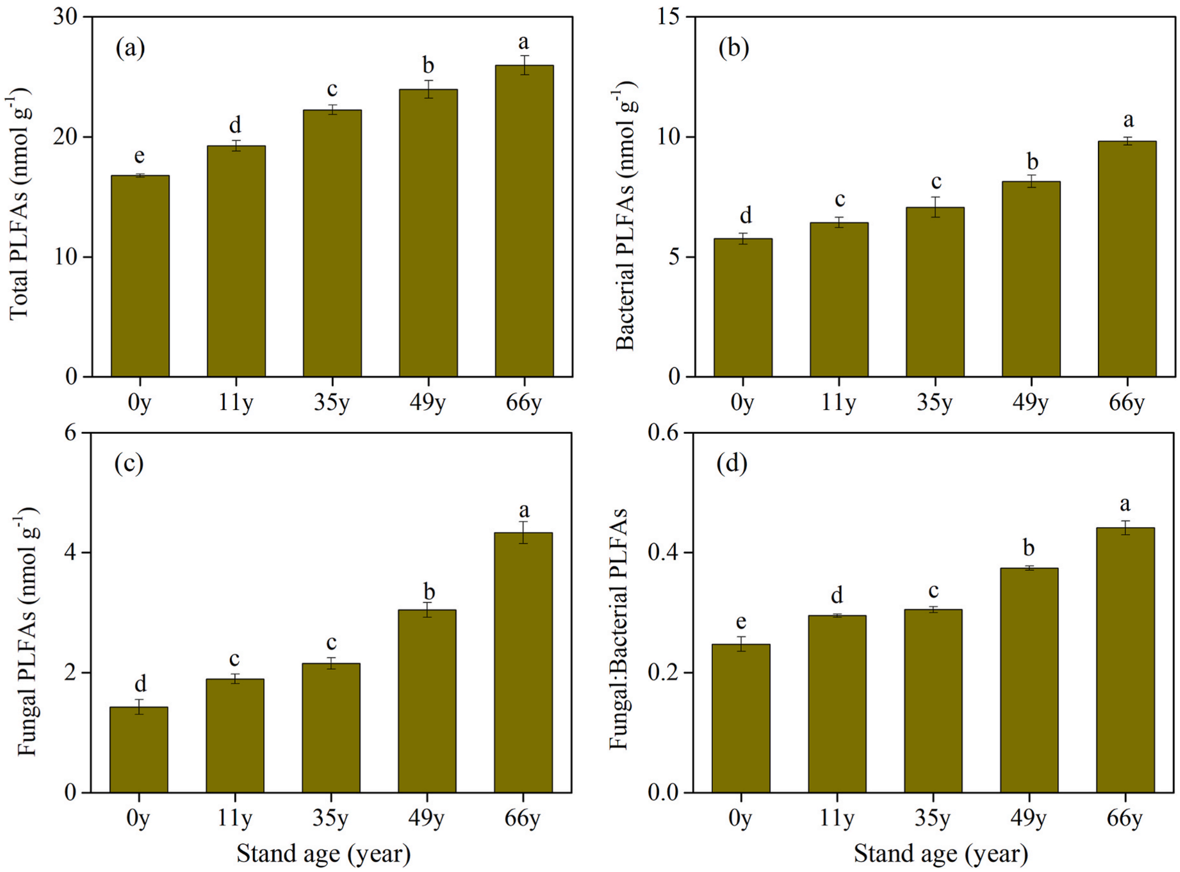

Fig. 3. Effect of revegetation on soil microbial community composition. Different letters indicate significant differences among stand age at $p < 0.05$.

also have confirmed that reforestation has considerable C sequestration capacity, and thus planting has a cooling effect by lowering atmospheric CO_2 concentration (Lewis et al., 2019). Additionally, revegetation in dryland promotes succession of floral communities and provides habitat for faunal communities. Our previous research showed that with the increase of revegetation age, the predominant plant gradually changed from perennial shrubs to annual herbaceous plants, and the number of species, coverage and biomass also increased significantly (Li et al., 2007, 2022a, 2022b).

On the other hand, the warming effects of revegetation have also long been recognized over large areas (Betts, 2000; Rohatyn et al., 2022). Revegetation changed the ground albedo, reduced shortwave radiation and increased net radiation and sensible heat flux, and thus creating local and potential global warming effects (Bonan, 2008). Especially in some dryland regions, the warming effect of albedo caused by revegetation may even be stronger than the cooling effect of C sequestration, because bright desert land turns to darker dense vegetation cover after revegetation (Rotenberg and Yakir, 2010). Furthermore, revegetation can also lead to loss of species that are well-adapted to the less-vegetated habitat. However, these are specialist species that are endemic or rare, especially in sand dunes (Provoost et al., 2011; Darke et al., 2013; Anglister et al., 2019). For instance, *Agriophyllum squarrosum* is a nutritious, adaptable and medicinal plant that dominates sand dunes, but it disappeared from the revegetated sites that we monitored over time (Li et al., 2016, 2022a, 2022b). Moreover, the changes in floral communities also have a non-negligible impact on faunal communities. A recent study demonstrated that the disappearance of psammophile rodents was closely link to the stabilization of mobile dunes and the presence of *Acacia saligna*, an invasive species brought to Israel for the purpose of dune stabilization (Anglister et al., 2019).

4.1. Effect of revegetation on MAOC

In general, the dynamics of SOC depend on the relationship between soil C input and output (Davidson and Janssens, 2006; Crowther et al., 2016; Zhu et al., 2017), and this relationship tends toward an equilibrium in a stable ecosystem in the long term (Harden et al., 2018). Revegetation can create novel ecosystems which are in continuous succession during the initial phase. Consequently, revegetation not only changes soil properties, plant inputs, and the soil microbial community but also interrupts the established equilibrium and leads to new SOC dynamics which may require decades, or even centuries, to reach a new equilibrium (Hong et al., 2020). The total SOC content increased significantly with site age, along with the MAOC content and proportion (Fig. 3), indicating that revegetation not only promoted the accumulation of total SOC but also increased the contribution of MAOC to the total SOC.

In this study, the clay and silt content strongly affected the MAOC proportion (Table 2), which was consistent with the findings of Haddix et al. (2020) and Yu et al. (2022). In another study, revegetation altered the soil formation environment and increased dust deposition (<0.063 mm); dust was the main material transported to the soil (Reynolds et al., 2001; Li et al., 2006), which had an important impact on soil development and particle composition in the revegetation area. The accumulated dustfall on sand the dune surface formed a protective layer and stabilized the sand surface, providing favorable conditions for soil formation and development (Yaalon and Ganor, 1973). Dustfall is rich in nutrients such as P, Mg, Na, and K and effectively increases soil fertility (Reynolds et al., 2001), which in turn affects plant community composition and productivity. Throughout the chronosequence, the clay and silt contents notably increased (Table 1), which might facilitate an increase in MAOC because clay and silt can protect MAOC from rapid decomposition by binding to the mineral surfaces (Lugato et al., 2021).

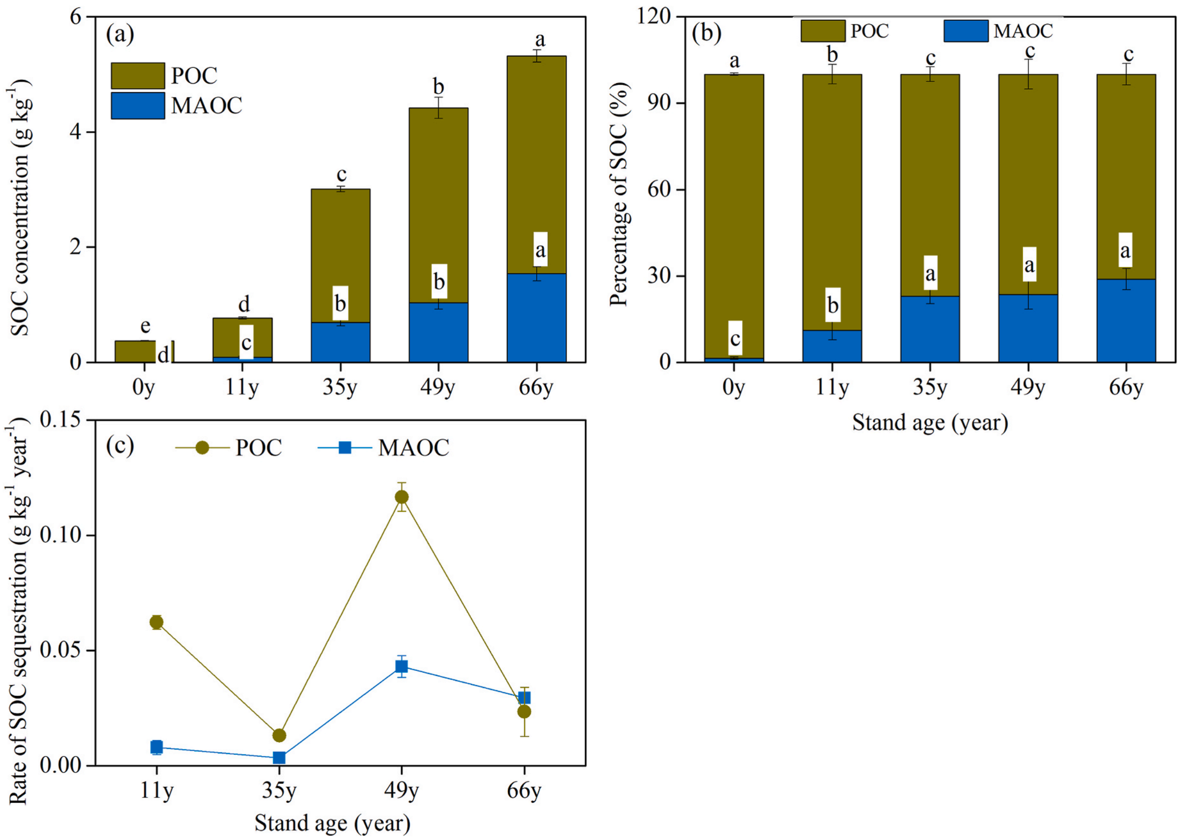

Fig. 4. Effect of revegetation on the concentration and distribution of MAOC and POC. Different letters indicate significant differences among stand age at $p < 0.05$.

Table 2
Pearson correlation coefficients (r) between MAOC, POC and proportion of MAOC and plant input, soil variables, and soil microbial community.

	Properties	MAOC	POC	PMAOC
Plant input	Litter mass	0.911**	0.931**	0.924**
	Fine root biomass	0.747**	0.788**	0.849**
Soil variables	Clay and silt content	0.960**	0.994**	0.943**
	Sand content	−0.960**	−0.994**	−0.943**
	SOC	0.995**	0.972**	0.907**
	TN	0.954**	0.980**	0.919**
	TP	0.947**	0.950**	0.867**
	BD	−0.947**	−0.954**	−0.882**
	C:N	0.905**	0.782**	0.823**
Soil microbial community	Total PLFAs	0.976**	0.934**	0.916**
	Bacterial PLFAs	0.976**	0.934**	0.916**
	Fungal PLFAs	0.899**	0.936**	0.812**
	F:B	0.911**	0.936**	0.839**

Note: Significant differences are marked as **, $p < 0.01$; *, $p < 0.05$. SOC, soil organic carbon; TN, total nitrogen; TP, total phosphorus; BD, bulk density; F:B, Fungal: Bacterial PLFAs, PMAOC, proportion of MAOC in bulk soil.

With increasing site age, soil texture and nutrient conditions become progressively more suitable for plant growth. As the soil BD decreased, the levels of TN and TP gradually increased (Table 1), providing nutrients for plant growth and consequently increasing the levels of SOC and MAOC (Fig. 2). Soluble constituents of plant litter are preferentially adsorbed to minerals (Kalbitz and Kaiser, 2008; Kramer et al., 2012). Moreover, the increase in litter mass and fine root biomass may also be an important factor for the increase in MAOC, and plant-derived C largely contributes to MAOC (Coward et al., 2018; Huang et al., 2019; Angst et al., 2021; Yu et al., 2022).

The variations in the microbial community also had a clear effect on MAOC accumulation in the revegetated sites, most likely because of the differences in the degradability of tissues and the ability of microorganisms to degrade organic matter (Liu et al., 2018). In this study, the soil fungal: bacterial PLFAs were significantly higher in older sites than in other sites (Fig. 3), indicating that the decomposition stage of soil organic matter was shifted form the early stage to the late stage with the increase of stand age. Therefore, the formation and accumulation of MAOC was accelerated, and MAOC was predominantly formed from low-molecular-weight compounds derived from the decomposition of labile plant inputs (Cotrufo et al., 2013; Lugato et al., 2021). Notably, the increase in MAOC may be closely related to the increase in the POC level. As POC generally decomposes more rapidly than MAOC (Parton et al., 1987; Feng et al., 2016), it also has a shorter retention time (Kleber et al., 2015). The nutrients and energy released during the decomposition of POC have fully met the needs of microbial growth. Therefore, from the perspective of microbial nutrient acquisition, there is no need to degrade a large amount of MAOC to obtain the nutrients needed for growth of microorganism, which is conducive to the accumulation of MAOC.

4.2. Effect of revegetation on POC

The POC level increased with increasing site age, which can be attributed to the considerable increase in plant input (Fig. 2). The litter and fine root biomass values in the 0-year-old site were negligible, whereas in the 66-year-old site, these values were 10.11 and 2.69 g m^{-2}, respectively (Fig. 2). The increase in litter and fine root biomass was the main driver of POC, which is mainly composed of structural polymeric compounds of plant origin (Baldock and Skjemstad, 2000); these compounds have a relatively short lifespan, with an average residence time in the range of years to decades (von Lützow et al., 2007).

More interestingly, the proportion of POC decreased with increasing site age, suggesting that the pattern of SOC accumulation changed from POC to MAOC. The decrease in the proportion of POC was related to soil

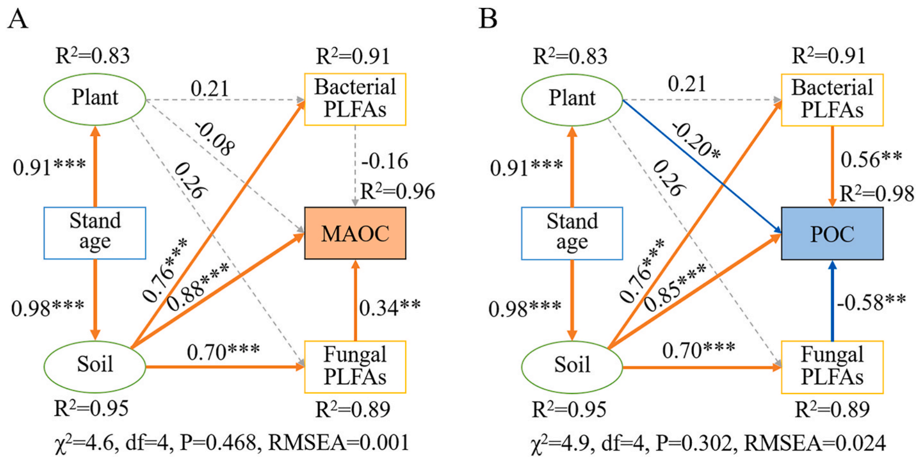

Fig. 5. Structural equation modeling (SEM) analysis examining the effect of stand age, plant, soil, and microbial biomass on the MAOC and POC. The ellipse represents the latent variable, the model of latent variable is shown in Fig. S1, the rectangle represents the observed variable. Single-headed arrows indicate the hypothesized direction of causation. Orange arrows indicate positive relationships and blue arrows indicate negative relationships. Width of arrows represent the strength of the relationship. The numbers next to arrows are standardized path coefficients. The solid represent significant (****p* < 0.001, ***p* < 0.01, **p* < 0.05) and the dashed represent non-significant (*p* > 0.05). The proportion of variance explained (R^2) appears alongside each response variables in the model.

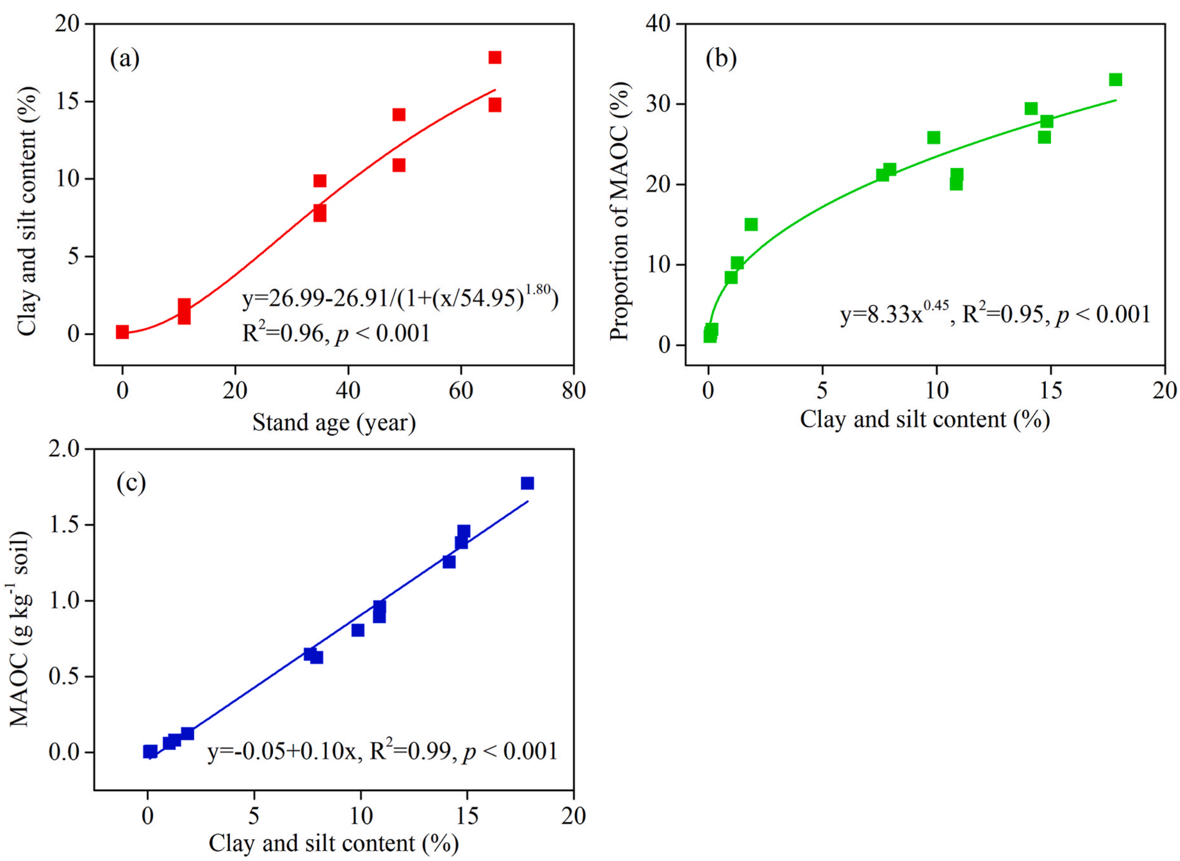

Fig. 6. Prediction of the effect of revegetation on the distribution of MAOC using the predictor of clay and silt content.

texture. The clay and silt content increased by 130.67 times after 66 years of revegetation (Table 1), which significantly increased the content and percentage of MAOC, thus decreasing the POC proportion. Moreover, the development and formation of BSCs are not conductive to the formation and accumulation of POC. According to a previous study, the development of BSCs is enhanced by revegetation (Li et al., 2000, 2006). Although BSCs can increase the survival rate of shrub seedlings due to reduced soil erosion (Li et al., 2006), they inhibit the entry of organic matter (e.g., litter) into the soil. After the degradation of the organic matter on the soil surface, only low-molecular-weight compounds and dissolved C could be transported to the soil layer beneath the BSCs, where they are preferentially adsorbed on the mineral particles to form MAOC (Kramer et al., 2012; Hall et al., 2020). This explains the decrease in POC proportion with increasing site age. The changes of litter quality may also be another reason for the decreased proportion of POC. A previous study in our study sites implied that the litter quality improved with site age (Li et al., 2023). Based on the MEMS hypothesis (Cotrufo et al., 2013; Liang et al., 2017), high-quality litter is more efficiently converted into microbial biomass and necromass and forms organo-mineral associations that accumulate in the soil (Cotrufo et al., 2013; Lavallee et al., 2018).

In the present study, the standardized path coefficients for the effects of bacterial and fungal PLFAs on POC content assessed by SEM were 0.56 and 0.58, respectively (Fig. 5b). Bacterial PLFAs were significantly positively correlated with POC, whereas fungal PLFAs were significantly negatively correlated with POC (Fig. 5b). Traditionally, the easily degradable C has been considered primarily bacterial, while recalcitrant substrates was considered to be dominated by fungi (Hunt et al., 1987; Wardle et al., 2004). Bacterial and fungal PLFAs increases with the increase of POC, which is considered to drive short-term SOC decomposition and it is mostly plant-derived (Yu et al., 2022). However, the increase in the fungal PLFAs accelerated the decomposition of recalcitrant components in POC, so the fungal PLFAs was negatively correlated with POC. In addition, the microbial numbers significantly increased with site age (Fig. 3); consequently, their requirements of C also increased, which in turn increased the consumption of POC. As POC is not protected physically or chemically by soil minerals, it is more easily degraded by microorganisms than MAOC (Cotrufo et al., 2019; Georgiou et al., 2022), which makes it the main driver of heterotrophic respiration (Elliott, 1986; Arevalo et al., 2012). Therefore, the increase in microbial abundance may be another important reason for the decreasing POC proportion over time.

4.3. *Effect of revegetation on SOC storage and stability*

Revegetation significantly increased the SOC content, and this effect was dependent on site age (Table 1). This information, however, does not provide a valid estimate of SOC stability, which can be better reflected by the relative distribution of MAOC and POC. In the study, MAOC and POC showed the same dynamics along the chronosequence, although their proportions showed different trends (Fig. 4). Whilst the POC dominated in all sites, the proportion of MAOC gradually increased with site age (Fig. 4). This leads us to infer that revegetation gradually improved the stability of SOC, which was dependent on site age.

In our previous study, we showed that the content of clay and silt was 13.67%–26.99% in the native vegetation area (Li et al., 2020a). In the present study, we estimated the maximum content and proportion of MAOC based on the linear relationship between clay and silt content and site age; the results showed that the maximum value of clay and silt content would be 27% in the 0–10-cm soil layer, and the MAOC content and proportion would reach maximum levels of 2.65 g kg^{-1} and 36.71%, respectively (Fig. 6). The content and percentage of MAOC reached 58.11% and 78.78%, respectively, of the maximum values after 66 years of revegetation. Although the SOC was still dominated by POC, our findings indicate that with ongoing vegetation succession, MAOC will continue to increase. Therefore, the stability of SOC in the sand-fixing vegetation area will increase over time.

Revegetation is considered an effective way to increase C sequestration and mitigate climate change (IPCC, 2014; Li et al., 2020b; Piao et al., 2020), resulting in an increased C storage in biomass and soil (Yao et al., 2018; Piao et al., 2020). Our result also suggests that vegetation succession also increased the content and stability of SOC; however, this effect was strongly correlated with soil texture. Our results highlight a promising model for improving the potential of SOC stability through improved soil texture by sound management practices.

5. Conclusions

Both MAOC and POC have been regarded as reliable indicators of the stability of SOC in recent years. Therefore, quantitative data are needed to determine the contribution of MAOC and POC to SOC storage in restored ecosystems. We expect that the contribution of MAOC to SOC will increase gradually and eventually reach a steady state with vegetation succession on mobile sand dunes. In the present study, revegetation significantly increased SOC storage, and the stability of SOC was enhanced by the changes in the proportions of MAOC and POC. The MAOC and POC contents largely depend on the plant input, soil properties, and the soil microbial community. The proportion of MAOC gradually increased with site age, whilst that of POC gradually decreased. This indicates that revegetation positively affects the storage and stability of SOC, governed by site age. We estimated that the maximum values of the content and proportion of MAOC will increase to 2.65 g kg^{-1} and 36.71%, respectively. This suggests that although revegetation improved the stability and storage of SOC, the soil sequestration potential is still high. Our results deepen our understanding of the functions of MAOC and POC in desert ecosystems. We highlight the importance of the revegetation of temperate desert ecosystems to increase the storage and stability of SOC and further mitigate global change.

Declaration of competing interest

The authors declare that they have no known competing financial interests or personal relationships that could have appeared to influence the work reported in this paper.

Data availability

The authors do not have permission to share data.

Acknowledgements

We gratefully thank Prof. Tim Clough and the anonymous reviewers for their constructive comments for improving the manuscript. This study was supported by the Foundation of Ningxia Independent Innovation on Agriculture Science and Technology (NGSB-2021-14-04), and the Key Research and Development Program of Ningxia Hui Autonomous Region (2022BEG03049).

Appendix A. Supplementary data

Supplementary data to this article can be found online at https://doi.org/10.1016/j.soilbio.2023.109155.

References

Abiodun, B.J., Adegoke, J., Abatan, A.A., Ibe, C.A., Egbebiyi, T.S., Engelbrecht, F., Pinto, I., 2017. Potential impacts of climate change on extreme precipitation over four African coastal cities. Climatic Change 143, 399–413.

Alvarez, R., Alvarez, C.R., 2000. Soil organic matter pools and their associations with carbon mineralization kinetics. Soil Science Society of America Journal 64, 184–189.

Anglister, N., Yom-Tov, Y., Motro, U., 2019. The impact of Acacia saligna and the loss of mobile dunes on rodent populations: a case study in the Ashdod-Nizzanim sands in Israel. Israel Journal of Plant Sciences 66 (3–4), 162–169.

Angst, G., Mueller, C.W., Prater, I., Angst, Š., Frouz, J., Jílková, V., Peterse, F., Nierop, K.G.J., 2019. Earthworms act as biochemical reactors to convert labile plant compounds into stabilized soil microbial necromass. Communications Biology 2, 1–7.

Angst, G., Mueller, K.E., Nierop, K.G.J., Simpson, M.J., 2021. Plant- or microbialderived? A review on the molecular composition of stabilized soil organic matter. Soil Biology and Biochemistry 156, 108189.

Arevalo, C., Chang, S., Bhatti, J.S., Sidders, D., 2012. Mineralization potential and temperature sensitivity of soil organic carbon under different land uses in the Parkland region of Alberta, Canada. Soil Science Society of America Journal 76, 241–251.

Bachelet, D., Neilson, R.P., Lenihan, J.M., Drapek, R.J., 2001. Climate change effects on vegetation distribution and carbon budget in the United States. Ecosystems 4 (3), 164–185.

Baldock, J.A., Skjemstad, J.O., 2000. Role of the soil matrix and minerals in protecting natural organic materials against biological attack. Organic Geochemistry 31, 697–710.

Bastin, J.F., Finegold, Y., Garcia, C., Mollicone, D., Rezende, M., Routh, D., Zohner, C.M., Crowther, T.W., 2019. The global tree restoration potential. Science 365 (6448), 76–79.

Betts, R.A., 2000. Offset of the potential carbon sink from boreal forestation by decreases in surface albedo. Nature 408 (6809), 187–190.

Bonan, G.B., 2008. Forests and climate change: forcings, feedbacks, and the climate benefits of forests. science 320 (5882), 1444–1449.

Bossio, D.A., Scow, K.M., 1998. Impacts of carbon and flooding on soil microbial communities: phospholipid fatty acid profiles and substrate utilization patterns. Microbial Ecology 35 (3), 265–278.

Cambardella, C.A., Elliott, E.T., 1992. Particulate soil organic-matter changes across a grassland cultivation sequence. Soil Science Society of America Journal 56, 777–783.

Chaturvedi, R.K., Gopalakrishnan, R., Jayaraman, M., Bala, G., Joshi, N.V., Sukumar, R., Ravindranath, N.H., 2011. Impact of climate change on Indian forests: a dynamic vegetation modeling approach. Mitigation and Adaptation Strategies for Global Change 16 (2), 119–142.

Christensen, B.T., 1987. Decomposability of organic matter in particle size fractions from field soils with straw incorporation. Soil Biology and Biochemistry 19, 429–435.

Christensen, B.T., 1996. Matching measurable soil organic matter fractions with conceptual pools in simulation models of carbon turnover: revision of model structure. In: Powlson, D.S., Smith, P., Smith, J.U. (Eds.), Evaluation of Soil Organic Matter Models Using Existing Long-Term Datasets. Springer-Verlag, Berlin, pp. 141–159.

Cotrufo, M.F., Wallenstein, M.D., Boot, C.M., Denef, K., Paul, E., 2013. The Microbial Efficiency-Matrix Stabilization (MEMS) framework integrates plant litter decomposition with soil organic matter stabilization: do labile plant inputs form stable soil organic matter? Global Change Biology 19, 988–995.

Cotrufo, M.F., Ranalli, M.G., Haddix, M.L., Six, J., Lugato, E., 2019. Soil carbon storage informed by particulate and mineral-associated organic matter. Nature Geoscience 12, 989–994.

Coward, E.K., Ohno, T., Plante, A.F., 2018. Adsorption and molecular fractionation of dissolved organic matter on iron-bearing mineral matrices of varying crystallinity. Environ. sci. technol. 52, 1036–1044.

Crowther, T.W., Todd-Brown, K.E., Rowe, C.W., Wieder, W.R., Carey, J.C., Machmuller, M.B., Snoek, B.L., Fang, S., Zhou, G., Allison, S.D., Blair, J.M., Bridgham, S.D., Burton, A.J., Carrillo, Y., Reich, P.B., Clark, J.S., Classen, A.T., Dijkstra, F.A., Elberling, B., Emmett, B.A., Estiarte, M., Frey, S.D., Guo, J., Harte, J., Jiang, L., Johnson, B.R., Kröel-Dulay, G., Larsen, K.S., Laudon, H., Lavallee, J.M., Luo, Y., Lupascu, M., Ma, L.N., Marhan, S., Michelsen, A., Mohan, J., Niu, S., Pendall, E., Peñuelas, J., Pfeifer-Meister, L., Poll, C., Reinsch, S., Reynolds, L.L., Schmidt, I.K., Sistla, S., Sokol, N.W., Templer, P.H., Treseder, K.K., Welker, J.M., Bradford, M.A., 2016. Quantifying global soil carbon losses in response to warming. Nature 540 (7631), 104–108.

Cunningham, S.C., Metzeling, K.J., Mac Nally, R., Thomson, J.R., Cavagnaro, T.R., 2012. Changes in soil carbon of pastures after afforestation with mixed species: sampling, heterogeneity and surrogates. Agriculture, Ecosystems & Environment 158, 58–65.

Cyle, K.T., Hill, N., Young, K., Jenkins, T., Hancock, D., Schroeder, P.A., Thompson, A., 2016. Substrate quality influences organic matter accumulation in the soil silt and clay fraction. Soil Biology and Biochemistry 103, 138–148.

Darke, I.B., Eamer, J.B., Beaugrand, H.E., Walker, I.J., 2013. Monitoring considerations for a dynamic dune restoration project: pacific rim national park reserve, British Columbia, Canada. Earth Surface Processes and Landforms 38 (9), 983–993.

Davidson, E., Janssens, I., 2006. Temperature sensitivity of soil carbon decomposition and feedbacks to climate change. Nature 440, 165–173.

de Moraes Sá, J.C., Gonçalves, D.R.P., Ferreira, L.A., Mishra, U., Inagaki, T.M., Furlan, F. J.F., Morog, R.S., Florianih, N., Briedis, C., de Oliveira Ferreira, A., 2018. Soil carbon fractions and biological activity based indices can be used to study the impact of land management and ecological successions. Ecological Indicators 84, 96–105.

Elliott, E.T., 1986. Aggregate structure and carbon, nitrogen, and phosphorus in native and cultivated soils. Soil Science Society of America Journal 50, 627–633.

FAO-ISRIC-ISSS, 1998. World reference base for soil resources. In: Soil Resources Report No 84. FAO, Rome.

Feng, W., Shi, Z., Jiang, J., Xia, J., Liang, J., Zhou, J., Luo, Y., 2016. Methodological uncertainty in estimating carbon turnover times of soil fractions. Soil Biology and Biochemistry 100, 118–124.

Georgiou, K., Jackson, R.B., Vindušková, O., Abramoff, R.Z., Ahlström, A., Feng, W., Harden, J.W., Pellegrini, A.F.A., Polley, H.W., Soong, J.L., Riley, W.J., Torn, M.S., 2022. Global stocks and capacity of mineral-associated soil organic carbon. Nature Communications 13 (1), 1–12.

Golchin, A., Oades, J.M., Skjemstad, J.O., Clarke, P., 1994. Study of free and occluded particulate organic matter in soils by solid state ^{13}C CP/MAS NMR spectroscopy and scanning electron microscopy. Soil Research 32 (2), 285–309.

Griepentrog, M., Bodé, S., Boeckx, P., Hagedorn, F., Heim, A., Schmidt, M.W.I., 2014. Nitrogen deposition promotes the production of new fungal residues but retards the decomposition of old residues in forest soil fractions. Global Change Biology 20, 327–340.

Griscom, B.W., Adams, J., Ellis, P.W., Houghton, R.A., Lomax, G., Miteva, D.A., Schlesinger, W.H., Shoch, D., Siikamäki, J.V., Smith, P., Woodbury, P., Zganjar, C., Blackman, A., Campari, J., Conant, R.T., Delgado, C., Elias, P., Gopalakrishna, T., Hamsik, M.R., Herrero, M., Kiesecker, J., Landis, E., Laestadius, L., Leavitt, S.M., Minnemeyer, S., Polasky, S., Potapov, P., Putz, F.E., Sanderman, J., Silvius, M., Wollenberg, E., Fargione, J., 2017. Natural climate solutions. Proceedings of the National Academy of Sciences 114 (44), 11645–11650.

Haddix, M.L., Gregorich, E.G., Helgason, B.L., Janzen, H., Ellert, B.H., Cotrufo, M.F., 2020. Climate, carbon content, and soil texture control the independent formation and persistence of particulate and mineral-associated organic matter in soil. Geoderma 363, 114160.

Hall, S.J., Ye, C., Weintraub, S.R., Hockaday, W.C., 2020. Molecular trade-offs in soil organic carbon composition at continental scale. Nature Geoscience 13, 687–692.

Harden, J.W., Hugelius, G., Ahlström, A., Blankinship, J.C., Bond-Lamberty, B., Lawrence, C.R., Loisel, J., Malhotra, A., Jackson, R.B., Ogle, S., Phillips, C., Ryals, R., Todd-Brown, K., Vargas, R., Vergara, S.E., Cotrufo, M.F., Keiluweit, M., Heckman, K. A., Crow, S.E., Silver, W.L., DeLonge, M., Nave, L.E., 2018. Networking our science to characterize the state, vulnerabilities, and management opportunities of soil organic matter. Global Change Biology 24 (2), e705–e718.

Heckman, K., Hicks Pries, C.E., Lawrence, C.R., Rasmussen, C., Crow, S.E., Hoyt, A.M., von Fromm, S.F., Shi, Z., Stoner, S., McGrath, C., Beem-Miller, J., Berhe, A.A., Blankinship, J.C., Keiluweit, M., Marín-Spiotta, E., Monroe, J.G., Plante, A.F., Schimel, J., Sierra, C.A., Thompson, A., Wagai, R., 2022. Beyond bulk: density fractions explain heterogeneity in global soil carbon abundance and persistence. Global Change Biology 28, 1178–1196.

Hong, S., Yin, G., Piao, S., Dybzinski, R., Cong, N., Li, X., Wang, K., Peñuelas, J., Zeng, H., Chen, A., 2020. Divergent responses of soil organic carbon to afforestation. Nature Sustainability 3 (9), 694–700.

Huang, W., Hammel, K.E., Hao, J., Thompson, A., Timokhin, V.I., Hall, S.J., 2019. Enrichment of lignin-derived carbon in mineral-associated soil organic matter. Environ. Sci. Technol. 53, 7522–7531.

Hunt, H.W., Coleman, D.C., Ingham, E.R., Ingham, R.E., Elliott, E.T., Moore, J.C., Rose, S. L., Reid, C.P.P., Morley, C.R., 1987. The detrital food web in a shortgrass prairie. Biology and Fertility of Soils 3, 57–68.

Joergensen, R.G., 2021. Phospholipid fatty acids in soil—drawbacks and future prospects. Biology and Fertility of Soils 58, 1–6.

Kalbitz, K., Kaiser, K., 2008. Contribution of dissolved organic matter to carbon storage in forest mineral soils. Journal of Plant Nutrition and Soil Science 171, 52–60.

Kleber, M., Eusterhues, K., Keiluweit, M., Mikutta, C., Mikutta, R., Nico, P.S., 2015. Chapter One - mineral–organic associations: formation, properties, and relevance in soil environments. In: Sparks, D.L. (Ed.), Advances in Agronomy. Academic Press, Cambridge, Massachusetts, pp. 1–140.

Kögel-Knabner, I., Guggenberger, G., Kleber, M., Kandeler, E., Kalbitz, K., Scheu, S., Eusterhues, K., Leinweber, P., 2008. Organo-mineral associations in temperate soils: integrating biology, mineralogy, and organic matter chemistry. Journal of Plant Nutrition and Soil Science 171 (1), 61–82.

Kramer, M.G., Sanderman, J., Chadwick, O.A., Chorover, J., Vitousek, P.M., 2012. Longterm carbon storage through retention of dissolved aromatic acids by reactive particles in soil. Global Change Biology 18, 2594–2605.

Lal, R., 2001. Potential of desertification control to sequester carbon and mitigate the greenhouse effect. Climatic Change 51 (1), 35–72.

Lal, R., 2004. Soil carbon sequestration to mitigate climate change. Geoderma 123 (1–2), 1–22.

Lavallee, J.M., Conant, R.T., Paul, E.A., Cotrufo, M.F., 2018. Incorporation of shoot versus root-derived ^{13}C and ^{15}N into mineral-associated organic matter fractions: results of a soil slurry incubation with dual-labelled plant material. Biogeochemistry 137, 379–393.

Lavallee, J.M., Soong, J.L., Cotrufo, M.F., 2020. Conceptualizing soil organic matter into particulate and mineral-associated forms to address global change in the 21st century. Global Change Biology 26, 261–273.

Le Houérou, H.N., 2000. Restoration and rehabilitation of arid and semiarid mediterranean ecosystems in north Africa and west Asia: a review. Arid Soil Research and Rehabilitation 14, 3–14.

Lewis, S.L., Wheeler, C.E., Mitchard, E.T., Koch, A., 2019. Restoring natural forests is the best way to remove atmospheric carbon. Nature 568 (7750), 25–28.

Li, X.R., Zhang, J.G., Wang, X.P., Liu, L.C., 2000. Study on soil microbiotic crust and its influences on sand fixing vegetation in arid desert region. Acta Botanica Sinica 42, 965–970.

Li, X.R., Xiao, H.L., He, M.Z., Zhang, J.G., 2006. Sand barriers of straw checkerboards for habitat restoration in extremely arid desert regions. Ecological Engineering 28 (2), 149–157.

Li, X.R., He, M.Z., Duan, Z.H., Xiao, H.L., Jia, X.H., 2007. Recovery of topsoil physicochemical properties in revegetated sites in the sand-burial ecosystems of the Tengger Desert, northern China. Geomorphology 88, 54–265.

Li, X.R., Zhang, Z.S., Liu, Y.B., Li, X.J., Yang, H.T., 2016. Fundamental Ecohydrology of Ecological Restoration and Recovery in Sandy Desert Regions of China. Science Press in Chinese, China.

Li, W.B., Zhang, H.X., Huang, G.Z., Liu, R.X., Wu, H.J., Zhao, C.Y., McDowell, N.G., 2020. Effects of nitrogen enrichment on tree carbon allocation: a global synthesis. Global Ecology and Biogeography 29, 573–589.

Li, Y.F., Du, J., Zhang, X., Xie, T., Li, X.J., 2020a. Carbon mineralization of soil covered by different types of biological crusts in the southeastern fringe of the Tengger Desert. Acta Ecologica Sinica 40 (5), 1580–1589.

Li, Y., Piao, S., Chen, A., Ciais, P., Li, L.Z., 2020b. Local and teleconnected temperature effects of afforestation and vegetation greening in China. National Science Review 7 (5), 897–912.

Li, W.B., McDowell, N.G., Zhang, H.X., Wang, W.Z., Mackay, D.S., Leff, R., Zhang, P.P., Ward, N.D., Norwood, M., Yabusaki, S., Myers-Pigg, A.N., Pennington, S.C., Pivovaroff, A.L., Waichler, S., Xu, C.G., Bond-Lamberty, B., Bailey, V.L., 2022a. The influence of increasing atmospheric CO_2, temperature, and vapor pressure deficit on seawater-induced tree mortality. New Phytologist 235 (5), 1767–1779.

Li, X.J., Li, Y.F., Xie, T., Chang, Z.Q., Li, X.R., 2022b. Recovery of soil carbon and nitrogen stocks following afforestation with xerophytic shrubs in the Tengger Desert, North China. Catena 214, 106277.

Li, Y.F., Wang, Z.J., Shi, W.L., Yang, H.T., 2023. Litter quality modifies soil organic carbon mineralization in ecological restoration area. Land Degradation & Development 34 (6), 1806–1819.

Liang, C., Schimel, J.P., Jastrow, J.D., 2017. The importance of anabolism in microbial control over soil carbon storage. Nat. Microbiol. 2, 1–6.

Liu, Y.B., Zhao, L.N., Wang, Z.R., Liu, L.C., Zhang, P., Sun, J.Y., Wang, B.Y., Song, G., Li, X.R., 2018. Changes in functional gene structure and metabolic potential of the microbial community in biological soil crusts along a revegetation chronosequence in the Tengger Desert. Soil Biology and Biochemistry 126, 40–48.

Lugato, E., Lavallee, J.M., Haddix, M.L., Panagos, P., Cotrufo, M.F., 2021. Different climate sensitivity of particulate and mineral-associated soil organic matter. Nature Geoscience 14 (5), 295–300.

Nosetto, M.D., Jobbagy, E.G., Paruelo, J.M., 2006. Carbon sequestration in semi-arid rangelands: comparison of Pinus ponderosa plantations and grazing exclusion in NW Patagonia. Journal of Arid Environments 67 (1), 142–156.

IPCC climate change 2014: synthesis report. In: Pachauri, R.K., Meyer, L.A. (Eds.), 2014. Core Writing Team. IPCC.

Parton, W.J., Schimel, D.S., Cole, C.V., Ojima, D.S., 1987. Analysis of factors controlling soil organic matter levels in Great Plains grasslands. Soil Science Society of America Journal 51, 1173–1179.
Piao, S., Wang, X., Park, T., Chen, C., Lian, X.U., He, Y., Bjerke, J.W., Chen, A.P., Ciais, P., Tømmervik, H., Nemani, R.R., Myneni, R.B., 2020. Characteristics, drivers and feedbacks of global greening. Nature Reviews Earth & Environment 1 (1), 14–27.
Poeplau, C., Don, A., 2013. Sensitivity of soil organic carbon stocks and fractions to different land-use changes across Europe. Geoderma 192, 189–201.
Provoost, S., Jones, M.L.M., Edmondson, S.E., 2011. Changes in landscape and vegetation of coastal dunes in northwest Europe: a review. Journal of Coastal Conservation 15, 207–226.
Reynolds, R., Belnap, J., Reheis, M., Lamothe, P., Luiszer, F., 2001. Aeolian dust in Colorado Plateau soils: nutrient inputs and recent change in source. Proceedings of the National Academy of Sciences 98 (13), 7123–7127.
Rohatyn, S., Yakir, D., Rotenberg, E., Carmel, Y., 2022. Limited climate change mitigation potential through forestation of the vast dryland regions. Science 377 (6613), 1436–1439.
Rotenberg, E., Yakir, D., 2010. Contribution of semi-arid forests to the climate system. Science 327 (5964), 451–454.
Schimel, D.S., 2010. Drylands in the earth system. Science 327 (5964), 418–419.
Smith, J.U., Smith, P., Monaghan, R., MacDonald, A.J., 2002. When is a measured soil organic matter fraction equivalent to a model pool? European Journal of Soil Science 53, 405–416.
Sokol, N.W., Bradford, M.A., 2019. Microbial formation of stable soil carbon is more efficient from belowground than aboveground input. Nature Geoscience 12 (1), 46–53.
Sokol, N.W., Sanderman, J., Bradford, M.A., 2019. Pathways of mineral-associated soil organic matter formation: integrating the role of plant carbon source, chemistry, and point of entry. Global Change Biology 25 (1), 12–24.
von Lützow, M., Kögel-Knabner, I., Ekschmitt, K., Flessa, H., Guggenberger, G., Matzner, E., Marschner, B., 2007. SOM fractionation methods: relevance to functional pools and to stabilization mechanisms. Soil Biology and Biochemistry 39 (9), 2183–2207.
Wardle, D.A., Bardgett, R.D., Klironomos, J.N., Setala, H., van der Putten, W.H., Wall, D. H., 2004. Ecological linkages between aboveground and belowground biota. Science 304 (5677), 1629–1633.
Willers, C., Jansen van Rensburg, P.J., Claassens, S., 2015. Phospholipid fatty acid profiling of microbial communities—a review of interpretations and recent applications. Journal of Applied Microbiology 119 (5), 1207–1218.
Witzgall, K., Vidal, A., Schubert, D.I., Hoschen, C., Schweizer, S.A., Buegger, F., Pouteau, V., Chenu, C., Mueller, C.W., 2021. Particulate organic matter as a functional soil component for persistent soil organic carbon. Nature Communications 12 (1), 4115.
Yaalon, D.H., Ganor, E., 1973. The influence of dust on soils during the Quaternary. Soil Science 116 (3), 146–155.
Yang, H.T., Li, X.R., Wang, Z.R., Jia, R.L., Liu, L.C., Chen, Y.L., Wei, Y.P., Gao, Y.H., Li, G., 2014. Carbon sequestration capacity of shifting sand dune after establishing new vegetation in the Tengger Desert, northern China. Science of the Total Environment 478, 1–11.
Yang, H.T., Li, X.R., Yan, P.J., Li, Y.F., Ma, Q.L., 2020. Soil types and spatial distribution in Tengger Desert. Journal of Desert Research 40 (4), 154–162.
Yao, Y., Piao, S., Wang, T., 2018. Future biomass carbon sequestration capacity of Chinese forests. Science Bulletin 63 (17), 1108–1117.
Yosef, G., Walko, R., Avisar, R., Tatarinov, F., Rotenberg, E., Yakir, D., 2018. Large-scale semi-arid afforestation can enhance precipitation and carbon sequestration potential. Scientific Reports 8 (1), 996.
Yu, P.J., Han, K.X., Li, Q., Zhou, D.W., 2017. Soil organic carbon fractions are affected by different land uses in an agro-pastoral transitional zone in Northeastern China. Ecological Indicators 73, 331–337.
Yu, W., Huang, W., Weintraub-Leff, S.R., Hall, S.J., 2022. Where and why do particulate organic matter (POM) and mineral-associated organic matter (MAOM) differ among diverse soils? Soil Biology and Biochemistry 172, 108756.
Zhang, H.X., Li, X.R., Guan, D.X., Wang, A.Z., Yuan, F.H., Wu, J.B., 2021. Nitrogen nutrition addition mitigated drought stress by improving carbon exchange and reserves among two temperate trees. Agricultural and Forest Meteorology 311, 108693.
Zhu, J., Hu, H., Tao, S., Chi, X., Li, P., Jiang, L., Ji, C.J., Zhu, J.L., Tang, Z.Y., Pan, Y.D., Birdsey, R.A., He, X.H., Fang, J., 2017. Carbon stocks and changes of dead organic matter in China's forests. Nature Communications 8 (1), 1–10.